Acoustic Studies during Ground Testing of an Experimental Nuclear Rocket Engine

R. S. FAIRALL,* W. R. THOMPSON,† AND A. D. CORNELL‡
Aerojet Nuclear Systems Company, Sacramento, Calif.

The factors necessary to define the acoustic field resulting from ground testing of an experimental nuclear rocket engine were investigated in scale-model tests and at various reactor power levels of the 50,000 lb thrust XE-Engine. Approximately 500 acoustic measurements were made; over-all and spectral analyses were performed to provide data for evaluation of acoustic prediction techniques. The mechanical jet power of the combusting hydrogen-rich gas jet ranged up to 190 Mw; the average mechanical-power-to-acoustic-power efficiency was 0.32%, whereas the thermal-power-to-acoustic-power efficiency was 0.0023%. Acoustic power was enhanced by the combustion process in the octave bands centered at 50, 100, and 200 Hz. The predicted value of the over-all sound pressure level at engine full power operation was about 1 db higher than the measured value.

Nomenclature§

DINDX = directivity index, db
DNF = near-field index, db
DWALL = wall index, db
OAPW = over-all acoustic power, w
OAPWL = over-all power level, db re 10^{-13} w
OASPL = over-all sound pressure level, db re 0.0002 dynes/cm^2
OBPWL = octave-band power level, db re 10^{-13} w
OBSPL = octave-band sound pressure level, db re 0.0002 dynes/cm^2
R = distance, microphone to center of sound, ft
WMJET = duct exit gas (jet) mechanical power, w
WTHJET = jet thermal power, w
η = mechanical-to-total-acoustic power conversion efficiency
ηM = mechanical-to-acoustic power conversion efficiency
ηTH = thermal-to-acoustic power conversion efficiency

Introduction

DEVELOPMENT testing of the NERVA nuclear rocket engine is performed at the Nuclear Rocket Development Station (NRDS), Jackass Flats, Nevada. Reviews of the engine program and the specialized test facilities have been given by Schroeder[1] and Rice and Arnold.[2] This paper discusses sound pressures arising from exhaust-plume-generated acoustics and describes experimental scale-model studies conducted to define the factors that characterize such jet noise fields. Acoustic data for operation of the reactor at various power levels are presented as is an analytical model that best predicts measured results.

Presented as Paper 70-174 at the AIAA 8th Aerospace Sciences Meeting, New York, January 19–21, 1970; submitted March 2, 1970; revision received April 23, 1970. C. P. Robinson and B. Washburn of the Los Alamos Scientific Laboratory, and H. Steiner, Marshall Space Flight Center, provided invaluable assistance in test planning and analysis. Work was carried out under Contract SNP-1, sponsored by the Space Nuclear Propulsion Office, Cleveland Extension, under the direction of G. K. Sievers.

* Senior Engineering Specialist, Thermodynamics, Engineering Department.
† Senior Engineering Specialist, Thermodynamics, Engineering Department. Member AIAA.
‡ Manager, Engine Design Section, NERVA Engine Department.

§ All notation is in FORTRAN.

Background Information on Exhaust-Plume Acoustics

The prototype NERVA (XE) is a downward-firing engine that exhausts heated hydrogen into a duct designed to direct the gases away from the test stand for safe burning in the atmosphere. The duct components of the nuclear exhaust system (NES) consist of a vertical second-throat section, a 90° elbow turning section, and a horizontal straight steam-driven ejector section that terminates in an upward-pointing 45° elbow. The NES is located in a concrete vault with the discharge elbow extending through a sheet metal wall that maintains an inert atmosphere within the vault (Fig. 1).

Testing of XECF (a nonfueled engine assembly) in April 1968 resulted in slight but definite damage to the test stand structure from noise generated by the burning plume. This structure, as well as other large sheet-metal walls on the test stand, would certainly be required to sustain even more severe sound pressures during testing of the prototype engine with its high-temperature, high-mass-flow-rate exhaust jet.

A survey was conducted of related experience applicable to this problem. The acoustic field for a nuclear rocket nozzle exhausting directly to the atmosphere (KIWI B) was determined by Manhart et al.[3] In this case, the high-temperature nozzle gases (hydrogen or helium) were directed vertically upward into the atmosphere with exit velocities up to 20,000 fps; whereas the NES duct exhausts steam-cooled and diluted hydrogen at velocities up to about 6000 fps. These systems are therefore basically dissimilar.

Acoustic data on subsonic jets, with and without combustion, have been compiled by Lighthill[4] and Washburn and Fenstermacher.[5] However, the jets involved were much smaller than that from the NES duct, and combustion was either nonexistent or stable. Mayes and Lanford[6] and Overton[7] compiled data on the noise produced by rocket engine firing at thrust levels from 1000 to 1,000,000 lb. Grande and co-workers[8] considered the effect of directivity on scaling hot and cold jets as well as the characteristics of the noise spectra and total acoustic power. A comprehensive summary of directivity functions for subsonic jets (air and turbojet exhaust) as well as supersonic jets was prepared by Howes.[9] A review of these and other available references, however, indicates a dearth of information on parameters considered significant to the determination of sound pressures on the test stand, i.e., velocity distribution at the duct exit plane and subsequent momentum exchange in the atmosphere, the

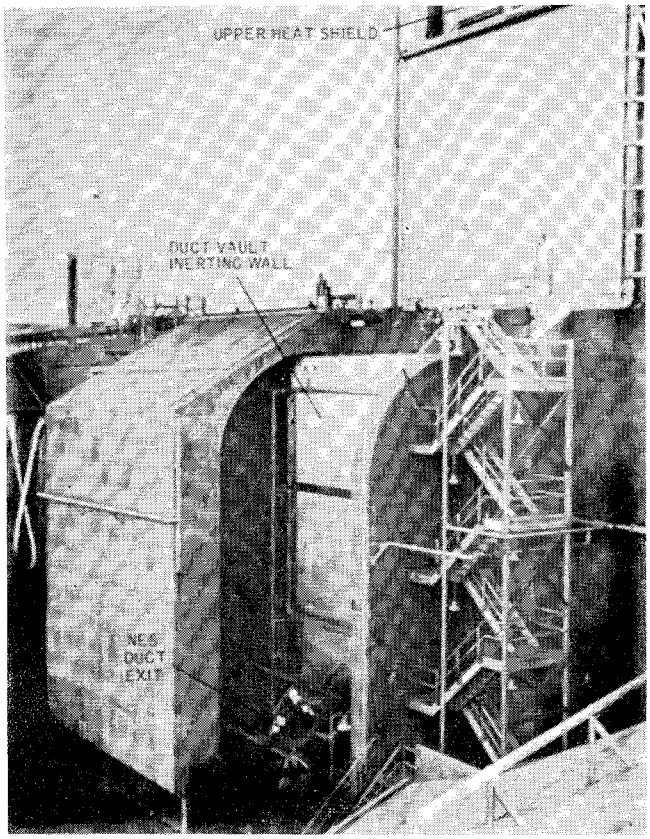

Fig. 1 NES duct exit and surrounding test stand structures, Engine Test Stand No. 1 (ETS-1).

effect of the state of mixing of engine hydrogen and ejector steam, and the limits and stability of diffusion combustion. Data from these different sources disagree by as much as 10 db.

A four-step experimental program was implemented using a $\frac{1}{8}$ scale model of the NES duct to: 1) define the acoustic field near the duct, 2) identify problem areas during partial-power runs, 3) correlate experimental acoustic data with predictions of various theoretical models and modify accordingly, and 4) identify and, if required, investigate evidence of oscillatory combustion. The model developed was then applied to predict exhaust plume acoustics for the XE test program.

Test Facilities

The $\frac{1}{8}$-linear-scale model includes Engine Test Compartment (ETC), supersonic diffuser, 90° subsonic turning elbow,

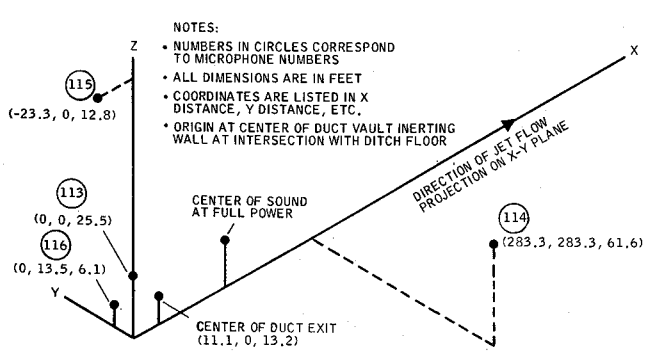

Fig. 2 Isometric sketch of coordinate system for microphone placement relative to NES duct exit and inerting wall.

Table 1 Microphone locations (scale model)

Microphone,[a] no. & type	Coordinates[b] X, ft	Y, ft	Z, ft	Distance,[c,d] ft	Angle,[e] deg
1 N	−1.5	0	0	3.33	4.57
2 N	−1.5	2	0.5	3.88	31.2
3 F	60	80	5	99.2	118.8
4 F	0	175	9	175.1	91.0
4 F	80	85	5	116.5	126.8
6 F	175	0	5	175.2	149.4
7 F	60	−80	5	99.2	−118.8

[a] N denotes near field, F far field.
[b] Coordinate system as shown in Fig. 2.
[c] Measured from the microphone to the calculated center of sound.
[d] Center of sound location estimated by the Dyer method for duct exit conditions of Test A5, Table 3.
[e] Measured from the forward end of a fictitious rocket having the same exhaust jet direction.

steam ejector, mixing section, and a 45° discharge elbow. It is provided with transducers to measure pressures in both the duct and the ETC. Measurements of the simulated engine and ejector gas temperatures are provided at three locations. The simulated engine (primary) and the ejector (secondary) gases are provided from high-pressure bottle storage via stored-energy heat exchangers. Hydrogen, nitrogen, and helium are available as primary and nitrogen as secondary gases. The upper temperature limit of the heat exchangers is 1500°R.

Hydrogen gas to the full-scale NES duct is provided by the engine at flow rates to 80 lb/sec. Steam, the ejector fluid, is provided from the combustion products of propane and oxygen as quenched with water. The term steam is used herein to conform with stand practice, but the fluid is not entirely steam, having a molecular weight of about 19. The upper temperature limit of the engine hydrogen exhaust is 4100°R, that of the steam generator products is 1660°R. The engine and facility control consoles are located in a blockhouse adjacent to the test stand. Flow rates and all other parameters are controlled through these consoles.

Six microphones were used in the scale-model study. These contained capacitive transducers that could measure static and dynamic pressures from 88 to 150 db re 0.0002 dynes/cm^2 at frequencies from 0 to 20,000 Hz. Two microphones (Photocon Model 404/2154) were designated near field and

Table 2 Scope of test data

	Species	Type of test
Scale model	H_2	Steady and ramp flow (including marginal combustion tests)
	N_2	Steady-flow
	He	Steady and ramp flow
XE	H_2	Transient-flow, EP-2A (bootstrap) and EP-6A (startup)
		Steady flow, EP-3A (intermediate power), EP-5C (full power), and EP-9A (high I_{sp})

	Scale model	XE
Primary gas:		
Species	N_2, H_2, and He	H_2
Flow rate, lb/sec	0–12.5	0–80
Temperature, °R	1200–1500	to 4100
Ejector gas:		
Species	N_2	steam
Flow rate, lb/sec	0–3.5	120–160
Temperature, °R	540–1200	540–1600
Duct geometry:		
Exit diameter, ft	0.532	4.33
Exit angle, deg	45	45

Table 3 Hydrogen scale-model flow parameters and sound pressure levels

Run no.	A2	A3	A4	A5	A6	(ramp rate is 6 psi/sec)		
Time, sec	10	10	10	10	23	52	67	92
Primary gas (H_2)[a]								
Flow rate, lb/sec	2.68	0.295	0.339	2.73	0.59	1.67	2.22	2.77
Total temperature, °R	1559	1373	1263	1555	1445	1508	1508	1504
Static pressure, psia	516	54	59	524	109	315	418	524
Secondary gas (N_2)								
Flow rate, lb/sec	None	None	3.37	3.51	None	None	None	None
Total temperature, °R	...	...	1225	1131	...	...	...	...
Static pressure, psia	...	...	117	117	...	...	...	...
Duct exit gas								
Flow rate, lb/sec	2.76	0.385	3.80	7.08	0.68	1.76	2.31	2.86
Total temperature, °R	1556	1355	1239	1510	1435	1504	1505	1502
Total pressure, psia	24.10	14.63	16.80	41.55	15.01	18.13	20.90	24.66
Molecular weight	2.079	2.575	12.922	4.664	2.298	2.116	2.092	2.077
Velocity, fps	5931	677	1174	4335	1457	3912	4985	5953
Mach number	0.88	0.11	0.47	1.00	0.22	0.57	0.74	0.91
Microphone SPL[b]								
No. 1	143	135	132	141	124	137	139	141
No. 2	143	135	132	141	124	139	139	139
No. 3	125	106	106	127	106	117	121	125
No. 5	123	106	107	125	104	115	119	124
No. 6	121	101	103	121	101	112	117	121
No. 7	123	103	105	124	103	115	120	124

[a] Includes bleed flow of N_2 at 0.09 lb/sec (540°R).
[b] SPL, sound pressure level, db re 0.0002 dynes/cm².

four (General Radio Model 1560-P5) were designated far field. Microphones were positioned as indicated in Table 1.

Four (Kaman Nuclear Model KM 1800-1) microphones were used in the full-scale study. Three were designated near field and were positioned at location numbers 113, 115, and 116 (Fig. 2). All were transducers capable of measuring static and dynamic pressures from 88 to 180 db re 0.0002 dynes/cm² at frequencies from 0 to 20,000 Hz. One was designated far field and positioned at location number 114. Preamplifiers were provided because of the long cables required. All microphones were supported by rubber shock-absorbing mountings to insure isolation from the support.

The sound pressure signals were amplified on facility amplifiers and recorded on magnetic tape. The final data playback was performed after the tests on a Bruel and Kjaer system for presentation either as over-all or octave-band sound pressure or in terms of frequency-spectrum pressure levels.

The tape playback unit was a Honeywell 7600. The signal from the tape was processed on a Bruel and Kjaer 221 Spectrometer; a true RMS Level Voltage Recorder was utilized for the over-all sound-pressure-level studies. For calibration, electrical and sound-wave signals were available. Electrical calibration was rejected as a primary calibration source for the microphones because of inability to calibrate the most questionable component in the system, the microphone itself. A General Radio Sound Level Calibrator, Type 1562-A, was selected for the sound source as a calibration standard.

Prior to scale-model tests, the near-field Photocon microphones were returned to the factory for a complete recalibra-

Table 4 Selected experimental engine (XE) flow parameters and sound pressure levels

Run no.	2A	2A	3	3	3	5C	5C	5C	5C	6A	9	9
t, sec	49350	49478	54625	54900	55250	38500	38800	38930	39200	44320	59200	59810
Engine GH_2												
$\dot{w}$, lb/sec	0	20.5	1.83	38.0	2.33	3.0	44.4	70.5	28.8	0	0	38.2
T_t, °R	...	1350	527	3050	1059	540	2380	4100	1956	...	...	3985
Turbine GH_2												
$\dot{w}$, lb/sec	0	1.97	0	4.26	0.10	0.10	4.43	7.37	2.70	0	0	3.68
T_t, °R	...	151	...	418	583	315	509	844	238	...	...	501
Bleed GH_2												
$\dot{w}$, lb/sec	6	6	6	6	1.61	1.61	1.61	1.61	1.61	0	0	0
T_t, °R	520	520	520	520	519	519	519	519	519	...	...	...
Steam												
$\dot{w}$, lb/sec	137.6	137.8	134.5	134.3	133.3	138.9	139.6	142.4	142.1	155.0	132.2	135.0
T_t, °R	1168	1203	1333	1359	1388	1350	1356	1358	1342	1275	1347	1371
Duct effluent												
$\dot{w}_{tot}$, lb/sec	143.6	165.8	142.3	183.2	141.7	143.7	190.0	221.9	175.2	155.0	132.2	176.9
$\dot{w}_{H_2}$, lb/sec	1.13	23.55	3.24	43.67	3.84	4.56	50.27	79.37	33.06	1.44	1.45	43.36
T_t, °R	1108	1110	1158	2111	1220	1168	1764	3053	1445	1215	1287	2659
Mol. wt.	19.84	9.14	19.39	6.52	17.36	16.41	6.04	4.78	7.55	19.50	19.38	6.37
γ	1.285	1.334	1.269	1.287	1.296	1.300	1.343	1.287	1.339	1.284	1.286	1.287
V, fps	423	1044	489	2960	556	542	2757	6395	1692	509	970	3643
Mach no.	0.225	0.372	0.243	0.671	0.263	0.254	0.647	1.000	0.484	0.257	0.330	0.732
Microphone SPL[a]												
HM-113	134.5	142.0	132.0	151.5	140.5	137.0	150.5	158.0	146.5	132.5	134.5	148.0
HM-114	112.5	121.0	109.5	123.0	112.5	112.0	125.0	132.4	[b]	108.5	112.0	126.5
HM-115	114.5	120.0	[b]	[b]	[b]	116.0	131.0	142.0	[b]	[b]	114.0	126.5
HM-116	125.7	144.0	136.5	149.6	140.0	138.0	148.5	156.2	144.5	135.0	135.0	148.5

[a] SPL, sound pressure level, db re 0.0002 dynes/cm².
[b] Electrical failure.

Table 5 Acoustic conversion efficiencies, selected scale-model tests

Test no.	A2	A2	A5	A5	A6	A6	A17	A17
microphone(s)	5	all	5	all	all	all	all	all
Time, sec	10	10	9	9	67	92	92	108
WMJET, Mw	2.03	2.03	2.79	2.79	1.204	1.204	0.640	0.207
OAPW, kw	8.12	11.77	10.32	9.49	4.70	5.54	2.94	0.869
OAPWL, db	159.3	170.8	170.2	159.7	166.6	167.4	164.7	169.4
η,%	0.40	0.58	0.37	0.34	0.39	0.46	0.46	0.42
ηM,%	0.20	0.20	0.20	0.20	0.20	0.20	0.20	0.20
ηTH,%	0.0023	0.0046	0.0027	0.0022	0.0017	0.0031	0.0024	0.0013

tion from 0 to 10,000 Hz and 60 to 150 db frequency range and sound pressure level. The test operation procedure required a pretest calibration from 125 to 2000 Hz at 115 db for each microphone; however, lateness of the hour or equipment demands sometimes forced deviations from this procedure. This procedure was restricted to the sound pressure measurements as other instruments are inherently more reliable and are calibrated periodically by facility personnel.

Method of Calculation

The ranges of duct operating parameters for the two experimental programs, scale model and XE, are summarized in Table 2. Typical data for the hydrogen scale-model experiments and the XE tests are presented in Tables 3 and 4, respectively, calculated as described below.

Flow processes in either duct can be visualized as adiabatic mixing of engine, turbine, and compartment purge gases at the duct inlet, flow with heat transfer through the diffuser and turning section, adiabatic mixing with ejector gas, flow with heat transfer through the ejector, and expulsion to the atmosphere. No chemical reaction is assumed in the duct. The one-dimensional duct exit velocity, mass flow rate, temperature, and pressure were calculated by application of the principles of conservation of energy and chemical species, continuity, and the equation of state.

Sound pressure levels were measured using microphones; jet mechanical power was calculated conventionally. Details are presented in Ref. 10. The expression for the mechanical-to-total-acoustic power conversion efficiency (η) was obtained from the measured sound pressure level, the calculated jet mechanical power, the measured distance, and the calculated directivity index. It was then assumed that the measured acoustic power equals the sum of the acoustic power due to jet-gas mechanical power and the jet-gas thermal power due to combustion. The thermal-to-acoustic power conversion efficiency (ηTH) was obtained from the calculated jet mechanical power, jet thermal power, total acoustic power conversion efficiency, and assumed mechanical-to-acoustic power conversion efficiency (ηM). The procedure is described below.

One ideal model of the acoustic process, the mechanical model, is applicable to all jets, and visualizes all the acoustic power as emanating from component power terms that are themselves proportional to the jet mechanical power; therefore, by this model,

$$\text{OAPW} = \eta\,(\text{WMJET}) \tag{1}$$

This equation can also be used as the definition of the total acoustic conversion efficiency.

Another ideal model of the acoustic proc ss, the thermal-mechanical model, is applicable only to burning jets, and visualizes all the acoustic power as emanating from two component power terms and is calculable as the sum of each taken separately. These two component terms are each assumed proportional to the jet mechanical power and the jet thermal power. By this model,

$$\text{OAPW} = (\eta\text{TH})(\text{WTHJET}) + (\eta\text{M})(\text{WMJET}) \tag{2}$$

From a rigorous viewpoint the thermal-mechanical model appears to offer the best approach; that is to say, the two component efficiencies should be more predictable than is the total acoustic efficiency.

Results of Data Analysis

Measured sound pressure levels are included in Tables 3 and 4. Acoustic conversion efficiencies for typical cases in both programs are presented in Tables 5 and 6. The average value of η [calculated from Eq. (1)] for all scale-model tests is 0.43% with a standard deviation of 0.074%. Similarly, the average value of ηTH [Eq. (2)] and its standard deviation are 0.0023 and 0.00099%, respectively. A constant value of ηM[¶] of 0.20% was assumed for all scale-model tests based on the data of Manhart.[3]

For all XE tests, the average values of η and ηM are 0.73 and 0.32%, respectively, with standard deviations of 0.254 and 0.181%, assuming a constant value of 0.0023% for ηTH [Eq. (2)]. The gross heating value of hydrogen was taken as 60,000 Btu/lb.

The somewhat lower standard deviation obtained using the thermal-mechanical model indicates improved prediction capabilities when the contribution of the combustion process to the total noise level is considered as an additive term to the mechanical contribution. Evaluation of the test results also confirms that for a duct using hydrogen gas mixtures a thermal-to-acoustic power conversion efficiency of 0.0023%, as calculated by Ortega,[11] would appear to be a valid number.

Table 6 Acoustic conversion efficiencies, selected engine tests (XE)

Test no. EP-	3	3	5C	5C	5C	6A
Time, sec	54625	54990	38800	38930	39200	44320
WMJET, Mw	0.714	16.8	30.3	191	10.5	0.843
OAPW, kw	6.03	111.5	201	1077	105.9	5.37
OAPWL, db	167.8	180.4	183.0	190.3	180.2	167.3
η,%	0.844	0.66	0.66	0.56	0.99	0.64
ηM,%	0.18	0.33	0.42	0.50	0.55	0.38
ηTH,%	0.0023	0.0023	0.0023	0.0023	0.0023	0.0023

¶ Where gas species were 100% hydrogen.

The calculated mechanical-to-total acoustic power conversion efficiency is in substantial agreement with the results of other investigators such as Manhart.[3]

The most important information obtained from this test series is the over-all sound pressure level (OASPL), as the structural integrity of the inerting wall is influenced by this parameter. Because jet noise is broadband in character, it is not necessary to analyze the noise in any great detail; over-all sound pressure levels and octave-band analysis, described later, are adequate. The over-all sound pressure levels were determined by tape playback on a Bruel and Kjaer analyzer and a summary of the results is shown in Tables 3 and 4. Pretest and post-test calibrations were utilized to range the analyzer and to insure that the calibration did not change during the test. Figure 3 shows typical over-all sound pressure levels for a burning hydrogen jet. Note that the duration of the test is important as the jet takes a finite time to reach steady-state.

All acoustic tapes were processed to obtain OBSPL (Octave-Band Sound Pressure Levels). The bands chosen for analysis were 25, 50, 100, 200, 400, 800, 1600, 3150, 6300, and 12,500 Hz. This narrow band analysis was done by using Bruel and Kjaer octave-band filters that have a relatively sharp cutoff, 13 db per $\frac{1}{3}$ octave. The results of the scale-model study for typical test conditions are also shown on Fig. 3. Note that there is a peak at about 100 Hz and another at about 1600 Hz that does not occur during tests with nitrogen or helium. It is suggested that the bi-modal spectra is typical of the hydrogen gas jet and the peak at the lower frequency is caused by combustion noise.

For the XE tests a preliminary estimate was made of the spectrum to determine the limits of the acoustic near and far fields of the jet tests. It was determined that a distance of 200 ft would be sufficient to insure that the microphones were located within the far field. Therefore, the far-field microphone was located more than 300 ft away from the sound center to insure that far-field results would be obtained. Microphones 113, 115, and 116 were intended to obtain specific design data in the near field and were located near the jet source on the critical components of the stand.

Errors (in db) in the OASPL and OAPWL values presented herein are estimated as follows: electrical noise, ±0.2; visual reading, ±1.0; data processing, ±0.5; acoustical calibration, ±0.1; roundoff error, ±0.5; and total probable (rss) error, ±1.25. For the Kaman and Photocon microphones this figure is accurate above 0.1 Hz; below that the response of the microphones falls off rapidly.

Figure 4 shows the relations between sound power and mechanical power for this and similar studies. The data shown for nuclear rockets are taken from Manhart[3]; those for chemical rockets are taken from Cole[12] and others as noted.

As would be expected from a study of previous results, calculations using the simple eighth power law of Lighthill,[4] which gives a good correlation for small, subsonic, cold-air jets, show that it does not appear applicable for large jets with high-velocity gases. The number of important parameters is probably much greater than in the case of a cold-air jet: gases of radically different molecular weight are mixing, the acoustic velocity in the jet is not the same as in the atmosphere, and the gas does not follow the 45° turn of the pipe elbow at the exit but turns only a fraction of that amount, to name only a few effects.

The mechanical power level of the jet when the engine is operating at design is about 400 times that at zero power. The ratio is not infinite because the steam is flowing, regardless of engine power, at about 130 lb/sec. The difference in efficiency is only 26%. This indicates a nearly constant efficiency in conversion of mechanical power to sound power over a wide range of thrust and power. This trend was demonstrated to extend over a range of jet mechanical power from 10^5 to 10^8 w. Other investigators have confirmed this trend.

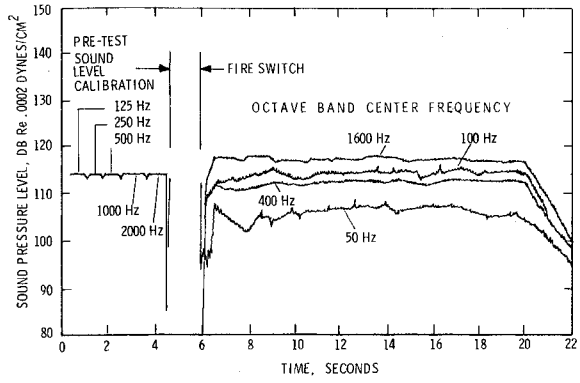

Fig. 3 Sound spectra for a burning hydrogen jet (scale Model Test A2, Microphone No. 3).

Combustion Studies

A scale-model test series was conducted (Tests A10 through A19) to determine 1) limits of combustion and 2) the acoustic field in this flammability limit region. It was important to know whether combustion, when it occurs, was steady or oscillating. Test data were obtained with duct effluent compositions ranging from 5 to 20 mole percent hydrogen. Infrared motion-pictures indicated that only a minimal amount of hydrogen, if any, burned. Based on a later evaluation of data on other jets, it appears that all five tests were made on the low side of the dynamic limit. Published dynamic data indicate lower flammability limits of 18 to 27 mole percent for the hydrogen-inerts effluent mixtures. Test data obtained from the scale-model tests show that the lower flammability limit is about 22 mole percent.

The test results (motion-picture film, magnetic tapes, personal observations, etc.) from each test were analyzed for any indication of oscillatory combustion. No evidence of this phenomenon was found.

Recommended Method

The objective of this investigation was to develop an acoustic prediction method suitable for this application (high-energy gas jets, near-sonic gas velocities, both near and far field, and large amounts of free hydrogen in the duct gas).

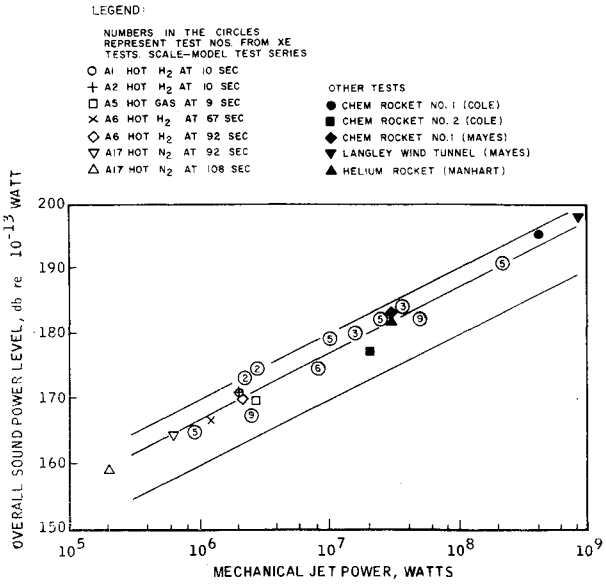

Fig. 4 Experimental relation of over-all sound power to jet mechanical power.

Accordingly, as soon as the preliminary results of the scale-model tests were complete, a preliminary model was developed. As engine test results became available, the theory was expanded and improved. The recommended prediction method is described below.

The jet kinetic and thermal power are calculated by conventional methods. The mechanical and thermal conversion efficiencies are estimated and over-all acoustic power is calculated from Eq. (2). The distance from the sound source and directivity index are estimated for the spectrum. The power spectrum levels are obtained by the method of Overton.[7] Wall and near-field effects are estimated from model tests. Octave band over-all sound pressure levels are calculated from

$$\mathrm{OBSPL} = \mathrm{OBPWL} - 10 \log (2\Pi R^2) + \mathrm{DINDX} + \mathrm{DNF} + \mathrm{DWALL} \quad (3)$$

$$\mathrm{OASPL} = 10 \log \sum_{i=1}^{M} \mathrm{antilog} \left(\frac{\mathrm{OBSPL}}{10} \right)_i \quad (4)$$

Restricting the discussion to the critical test condition, the agreement between the measured and predicted OASPL values for Run 5C for all four microphones is within ±1 db.

Conclusions

An experimental program to determine the acoustic characteristics of 0.5 and 4.3-ft-diam hot-gas jets exhausting to the atmosphere with mechanical jet power of up to 190 Mw and at an angle of about 40° to the horizontal has been completed. The gas-jet composition was varied but was substantially a mixture of H_2, N_2, and steam.** The characteristics of the sound field generated have been delineated and compared with those of other nuclear-rocket, chemical-rocket, cold-gas jets. Examination of the data shows that the sound field has the following characteristics.

1) The theoretical model described herein predicts the noise field resulting from power tests of the XE nuclear rocket engine in a satisfactory manner. The calculated value of over-all sound pressure level is about 1 db higher than the measured value.

2) A 0.32% mechanical-power-to-acoustic-power conversion efficiency and a 0.0023% thermal-power-to-acoustic-power conversion efficiency were obtained from an average of the engine test data. The mechanical-to-total-acoustic-power conversion efficiencies were about 0.73% and 0.44% for the engine and scale-model tests respectively.

3) Acoustic power was enhanced by the combustion process in the octave bands centered at 50, 100, and 200 Hz. Very little effect was noted at other frequencies.

4) The spectral shape for the jet noise field agrees quite well with that found by Overton[7] and the acoustic efficiency with Manhart.[3]

5) A predicted dynamic limit of flammability of about 22 mole percent hydrogen for the test conditions and geometry of this investigation was confirmed.

6) No evidence of oscillatory combustion was observed in any of the experiments.

7) Examination of the octave-band-sound pressure spectra for the steam and hydrogen full-power jet indicates about 5 db/octave roll-off below the frequency at which the sound pressure is maximum and a roll-off of about 2.5 db per octave above this frequency.

8) The probably accuracy of the individual measurements is estimated to result in an overall accuracy of ±1.25 db in the sound pressure levels calculated from the measurements.

9) The simple eight-power law of Lighthill[4] which gives good results for small, subsonic, cold-air jets is not applicable to large, hot, low molecular weight, near-sonic gas jets.

** Helium was included in the scale model but not the XE tests.

References

[1] Schroeder, R. W., "NERVA—Entering a New Phase," *Astronautics and Aeronautics*, Vol. 6, No. 5, May 1968, pp. 42–53.

[2] Rice, C. M. and Arnold, W. H., "Recent NERVA Technology Development," *Journal of Spacecraft and Rockets*, Vol. 6, No. 5, May 1969, pp. 565–569.

[3] Manhart, J. K. et al., "An Acoustical Study of the KIWI B Nuclear Rocket," CR-730, Jan. 1966, NASA.

[4] Lighthill, M. J., "Jet Noise," *AIAA Journal*, Vol. 1, No. 7, July 1963, pp. 1507–1517.

[5] Washburn, B. and Fenstermacher, C., "Acoustical Problem Survey and Recommendations," Test-Cell "C" Memorandum, Feb. 6, 1968, Los Alamos Scientific Lab., Los Alamos, N. Mex.

[6] Mayes, W. H. and Lanford, W. E., "Near Field and Far Field Noise Surveys of Solid Fuel Rocket Engines," TN D-21, Aug. 1959, NASA.

[7] Overton, J. B., "Methods for Establishing Noise Levels from a Missile Firing and Effects of These Noise Levels," NMC-TM-60-33, Aug. 1960, U.S. Navy Missile Center, Pt. Mugu, Calif.

[8] Grande, E., Large, J. B., and Anderson, A. D., "The Development of Engineering Practice in Jet and Compressor Noise," AIAA Paper 68-550, Cleveland, Ohio, 1968.

[9] Howes, W. L., "Similarity of Far Noise Fields of Jets," TR-R-52, 1960, NASA.

[10] Fairall, R. S., *An Acoustical Study of the Noise Field of the Jet from the ETS-1 Scale-Model NES Duct*, Rept. RN-TM-0579, Jan. 1969, Aerojet-General Corp., Sacramento, Calif.

[11] Ortega, J. C., *Acoustic Analysis Relating to ETS-1 Duct Vault Inerting Wall*, Paul S. Veneklasen and Associates, Santa Monica, Calif., Dec. 1968.

[12] Cole, J. N. et al., "Noise Radiation from Fourteen Types of Rockets in the 1000 to 130,000 Pounds Thrust Range," Rept. TR-57-354, 1957, Wright Air Development Center.